Optimal hydrologic regime for regenerating Fe^{III} electron acceptors for iron reduction in upland soils

Salvatore Calabrese[1], Diego Barcellos[2,3], Aaron Thompson[4], Amilcare Porporato[1]

[1]Department of Civil and Environmental Engineering and Princeton Environmental Institute, Princeton University, Princeton, NJ, USA.
[2]Escola Superior de Agricultura "Luiz de Queiroz", University of São Paulo, Piracicaba, SP, Brazil
[3]Department of Oceanography, Universidade Federal do Espírito Santo, Vitória, ES, Brazil
[4]Department of Crop and Soil Sciences, University of Georgia, Athens, GA, USA.

Key Points:

- The optimal oxic/anoxic cycle for iron (Fe) reduction is highlighted
- The oxic/anoxic cycle and Fe reduction are related to the soil moisture and rainfall variability
- Hydro-climate control on Fe reduction potential is studied in a tropical and a subtropical forest

Corresponding author: Salvatore Calabrese, sc58@princeton.edu

Abstract

In the predominantly oxic, upland soils, periods of high wetness trigger anaerobic processes such as iron (Fe) reduction within the soil microsites, with implications for organic matter decomposition, the fate of pollutants, and nutrient cycling. In fluctuating O_2 conditions, Fe reduction is maintained by the re-oxidation of ferrous iron, which renews the electron acceptor, Fe^{III}, for microbial Fe reduction. To characterize such processes, it is fundamental to relate the redox cycling of iron between the two redox states to the hydro-climatic conditions. Here, we link iron cycling to soil moisture variability through a model of iron-redox dynamics and find the hydrologic regime that maximizes Fe reduction, under non-limiting organic carbon availability. Away from the optimal cycle, the duration of the oxic or the anoxic phase limits the regeneration of Fe^{III} or its reduction rate, respectively. We relate the average duration of the oxic and anoxic intervals to the frequency and mean depth of precipitation events that drive the dynamics of soil moisture, effectively linking iron cycling to the hydrologic regime. We then compare a tropical (Luquillo CZO) and a subtropical (Calhoun CZO) forest to provide insights into the soil moisture control on iron-redox dynamics in these ecosystems. The tropical site maintains a high potential for iron reduction throughout the year, due to quick and frequent transitions between oxic and anoxic conditions, whereas the subtropical site is strongly affected by seasonality, which limits iron reduction to winter and early-spring months with higher precipitation and lower evaporative demand.

Plain Language Summary

Iron (Fe) plays a critical role in terrestrial ecosystems, influencing from the carbon cycle to the mobilization of contaminants and the formation of colloidal particles. It thus important to understand and quantify its biogeochemical cycle in relation to the environmental factors that drive it, for example the oxygen content in the soil pores. Here, we couple its redox cycle, consisting of Fe reduction and subsequent Fe oxidation, to the in-situ rainfall and soil moisture variability and show that the cycle is faster for a specific hydro-climate. These results represent an important step towards predicting the potential for iron redox cycling across different climate and identify the climatic regions where the Fe biogeochemical cycle may participate more actively in ecosystem functioning.

1 Introduction

The iron (Fe) biogeochemical cycle is an important component of terrestrial ecosystems, where it is implicated in the decomposition of the organic matter (E. Herndon et al., 2017; Bhattacharyya et al., 2018; Calabrese & Porporato, 2019; Vermeire et al., 2019; Han et al., 2019; Zheng et al., 2019; LaCroix et al., 2019), the formation of colloids (Stucki, 2011; Henderson et al., 2012; Wang et al., 2019) and mobilization of contaminants (Borch et al., 2009; Bishop et al., 2014; Couture et al., 2015; Yu et al., 2016). Predicting the variations in Fe reduction rates as a function of the hydro-climatic requires linking processes from the pedon to the watershed scale, but this has been challenging because of the numerous factors that affect the Fe redox chemistry.

The fundamental constraint on the Fe redox dynamics is the reduction of Fe^{III}, which has slower kinetics than the oxidation of Fe^{II} (Lovley, 1991; Ginn et al., 2017; Chen & Thompson, 2017). During anoxic conditions, Fe^{III}-reducing microorganisms rely on the availability of Fe^{III}-oxides as an electron acceptor, reducing it to ferrous iron (Fe^{II}) in order to decompose the organic matter (Lovley, 1991; Roden & Wetzel, 1996; Dubinsky et al., 2010). The rate of Fe^{III} reduction thus depends on a suitable organic substrate (LaRowe & Van Cappellen, 2011), the activity of Fe-reducers, as well as the abundance of Fe^{III} electron acceptor relative to other more thermodynamically favorable ones (e.g., O_2, Mn^{IV}).

The energy yield obtained from oxidizing organic matter coupled to Fe as electron acceptor is lower than the energy yield obtained when coupled to O_2. Thus, Fe reduction is strongly dependent upon the availability of an easily degradable substrate (LaRowe & Van Cappellen, 2011), whereas those substrates that require more energy to oxidize (i.e., have higher ΔG values for the C oxidation half reaction) can become thermodynamically unfavorable for microbial Fe^{III} reduction. The abundance and activity Fe-reducers is critical for predicting Fe reduction rates. Laboratory and field observations both have shown that Fe reduction is faster when the soil has experienced Fe reduction in the recent past (Buettner et al., 2014; Barcellos, Cyle, & Thompson, 2018), suggesting increased Fe-reducers activity in these conditions. Lastly, higher reduction rates are driven mostly by recently oxidized Fe^{II} (Weiss et al., 2004, 2005; Thompson et al., 2006). The availability of Fe^{III} electron acceptor can in fact be quantified through measurements of short range ordered Fe^{III} minerals.

The above arguments suggest that Fe reduction rates are strongly controlled by the characteristics of the soil oxic/anoxic cycles. In fact, in well-aerated soils (oxic conditions), iron mostly remains in its oxidized state (Fe^{III}) and aerobic respiration is the main mechanism of carbon decomposition, whereas in nearly constantly anoxic environments, such as wetlands or paddy soils, iron may persist in its reduced state (Fe^{II}) and other metabolisms typical of low redox potentials may be triggered, i.e., fermentation or methanogenesis (Morel et al., 1993; Brady & Weil, 2016). Between these extreme scenarios, a continuous transitions between oxic and anoxic conditions (e.g., wet tropical soils, river banks, fluctuating water tables), which spurs the formation of degradable organic substrates, higher activity of Fe reducers, and the continuous regeneration of Fe^{III}, may favor high rates of iron reduction (Calabrese & Porporato, 2019).

The main environmental factor controlling the transitions between oxic and anoxic conditions is the soil water content (Todd-Brown et al., 2012; Brady & Weil, 2016), as this determines the activity of aerobic bacteria and the fraction of air-filled volume. Experimental studies show that soil moisture may be a proxy for oxygen content, because this remains relatively high ($\approx 20\%$) for water contents up to the soil field capacity and then nonlinearly declines to $\approx 0\%$ as the soil approaches saturation (Hall et al., 2013; Barcellos, OConnell, et al., 2018). A quantification of the fate and redox changes of soil iron, necessary for the understanding of the global carbon cycle and related climate dynamics (Colombo et al., 2014; Oertel et al., 2016; Zheng et al., 2019), then needs to be carried out in relation to how hydro-climatic variability can induce changes in soil aeration and redox potential.

Towards this goal, we derive the relationship between the average Fe reduction rate and the length of exposure to oxic and anoxic conditions, which is related to the hydrologic regime. By means of a mechanistic iron-redox model, we explore the interaction between the timescales of the biogeochemistry (i.e., the reaction rates) and of the changes in environmental conditions (i.e., oxic/anoxic cycle) and highlight the existence of a maximum average Fe reduction rate at an intermediate anoxic/oxic intervals ratio. We then relate the oxic/anoxic cycle to the hydro-climatic fluctuations and link the characteristics of the cycle to the statistical properties of the soil moisture dynamics and precipitation, in terms of its frequency and mean rainfall depth. This effectively links iron reduction to the in-situ hydro-climatic variability, for which measurements are readily obtained through direct or remote sensing techniques. Applying the framework to soils from a humid tropical forest (Luquillo CZO) and a subtropical forest (Calhoun CZO), we explore the iron-redox dynamics in these different ecosystems and discuss its control on the carbon cycle and plant primary productivity.

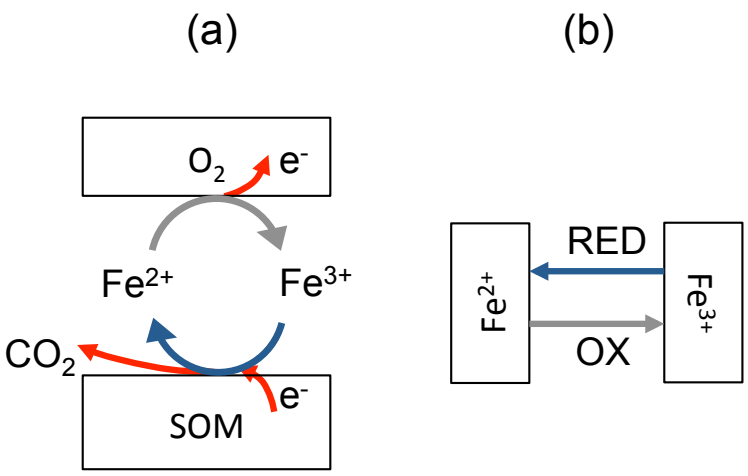

Figure 1. (a) Schematic representation of the soil iron cycle, emphasizing the electron transport from the soil organic matter (SOM) to the atmospheric oxygen by means of iron Fe^{II}, which operates as an 'electron carrier'. See description in Section 2. (b) Schematics of the iron redox cycle described by equation (1).

2 Optimal oxic/anoxic cycle for Fe reduction

The soil iron cycle, summarized in Figure 1(a), has an anoxic phase, in which Fe^{III} is utilized as an electron acceptor to decompose organic matter and an oxic phase, when oxygen oxidizes Fe^{II}, thus regenerating the Fe^{III} pool. Going back and forth between the two oxidation states, iron operates as an 'electron carrier' between the soil organic matter and the atmospheric oxygen (Figure 1 (a)), so that the decomposition depends on the rate at which electrons can be transported from the organic matter to oxygen. Decomposition by iron reduction in fact needs a continuous supply of iron Fe^{III}, which after having been reduced to Fe^{II} during a anoxic phase needs to be regenerated (i.e., re-oxidized) during the subsequent oxic phase. It is thus clear that the hydro-climate generating the oxic/anoxic cycles exerts a major control on the rate of iron cycling.

Consider the top soil layer containing organic matter and refer to the total iron content in the oxidized and reduced states as Fe^{II} and Fe^{III}, respectively. The total content of reducible iron is constant and equal to $Fe^{TOT} = Fe^{II} + Fe^{III}$. Since our focus is on the maximum rates, we assume that the availability of the organic substrate and microbes does not limit the reactions, so that the regeneration of Fe^{III} electron acceptor and presence/absence of anoxic conditions limit the reaction. The hydrologic cycle will thus govern the reaction rates in this framework. The soil is subject to an oxic/anoxic cycle of duration T that begins with the anoxic phase of duration $\tau_a = fT$ (Figure 2), whereas the oxic phase lasts for $\tau_o = (1-f)T$, f being the anoxic fraction. During the anoxic phase, only iron reduction occurs (no oxidation allowed), with a consequent increase of Fe^{II}. During the oxic phase, iron reduction stops and Fe^{II} is oxidized to Fe^{III} (Figure 1(b)). Such dynamics are described by the following mass balance equation,

$$\frac{dFe^{II}}{dt} = RED - OX, \tag{1}$$

where $RED = k_R(Fe^{TOT} - Fe)$ and $OX = k_O Fe^{II}$, k_R and k_O being the reduction and oxidation rate constants, respectively. Note that these expressions do not contain a dependence on the amount of substrate and microbial activity, as we are focusing exclusively on the hydrologic regime. However, the rate constants do explicitly depend on the time, t, in that during the anoxic phase $k_O = 0$, while during the oxic phase $k_R =$

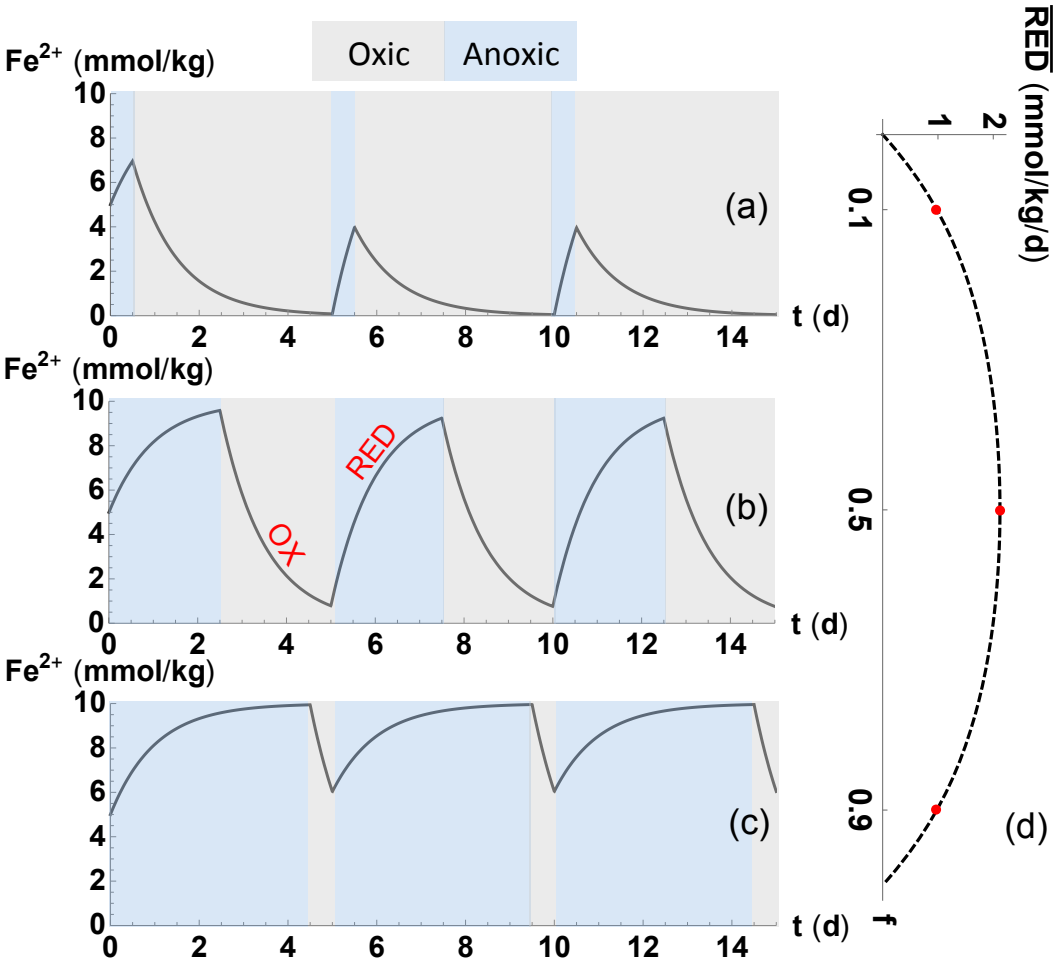

Figure 2. Time evolution of Fe^{II} content for different values of the ratio of anoxic/oxic intervals, $f = 0.1$ in (a), $f = 0.5$ in (b) and $f0.9$ in (c). The period of the anoxic/oxic cycle is fixed, $T = 5$ days. (d): (Dashed line) Average reduction rate, $R\bar{E}D = 1/T \int_T RED(t)dt$, as a function of f, for $T = 5$ days. (Red points) Average reduction rate for f equal to 0.1, 0.5, and 0.9.

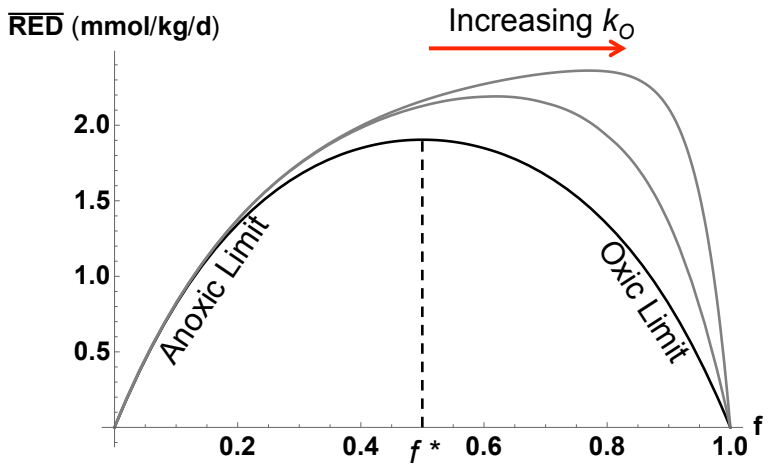

Figure 3. Average reduction rate, $\bar{RED} = 1/T \int_T RED(t)dt$, for different values of the reduction and oxidation rate constants, as a function of f and $T = 5$ days. The reduction rate constant $k_R = 1$ mmol/kg/d, while the oxidation rate constants are, from left to right, 1, 2 and 5 mmol/kg/d.

0. Solving equation (1) for sufficiently long time such that the initial condition has no longer influence, the stationary solution for a given oxic/anoxic cycle (shown in Figure 2(a)) is given by an exponential decay during the oxic phase,

$$Fe^{\mathrm{II}}(t) = Fe_0^{\mathrm{II}} e^{-k_O t}, \tag{2}$$

where Fe_0^{II} is the iron content at the end of the preceding anoxic phase and t is the time elapsed since the beginning of the oxic phase. On the contrary, during the anoxic phase Fe^{II} increases, approaching exponentially Fe^{TOT},

$$Fe^{\mathrm{II}}(t) = Fe^{TOT} - Fe_0^{\mathrm{II}'} e^{-k_O t}, \tag{3}$$

$Fe_0^{\mathrm{II}'}$ being the iron content at the end of the preceding oxic phase and t the time elapsed since the beginning of the anoxic phase.

In an extreme scenario, in which conditions are set to be always oxic ($f = 0$, Figure 2), iron content persists in its oxidized state, $Fe^{\mathrm{II}}(t) = 0$, and the average reduction rate, which can be defined as $\overline{RED} = 1/T \int_T RED(t)dt$, goes to zero. On the other hand, for a scenario of constant anoxic conditions ($f = 1$, Figure 2) iron persists in its reduced state, $Fe^{\mathrm{II}}(t) = Fe^{TOT}$, and again the reduction rate $\overline{RED} = 0$. This argument suggests that a maximum reduction rate $\overline{RED}^*$ exists at an intermediate value of f, f^*. Solving equation (1) for different values of f, the different $\mathrm{Fe^{II}}$ trajectories are shown in Figure 2, and computing the average reduction rate per cycle, see Figure 2(d), illustrates the anoxic/oxic cycle for which the $\overline{RED}$ is maximum.

The optimal f^* at which the maximum $\mathrm{Fe^{III}}$ is achieved depends on the reaction rate constants, k_R and k_O. For simplicity, Figure 2 demonstrates that, in the hypothetical condition in which $k_R = k_O$, the resulting $f^* = 0.5$. For higher k_R or k_O, shorter anoxic or oxic phases are needed to reduce or oxidize the same amount of iron, respectively. As the ratio of anoxic.oxic time moves away from the optimal f, the oxic/anoxic cycles is favoring either the reduction ($f > f^*$) or the oxidation ($f < f^*$), leading to an inhibition of Fe cycling. When $f > f^*$, the iron-redox cycle is limited by the regeneration of $\mathrm{Fe^{III}}$ electron acceptor, as essentially there is not enough time to oxidize enough sufficient iron to use in the following anoxic phase. On the contrary, when $f < f^*$ the iron-redox cycle is limited by the $\mathrm{Fe^{III}}$ reduction, such that the anoxic phase is too short to reduce substantial amounts of iron (Figure 3).

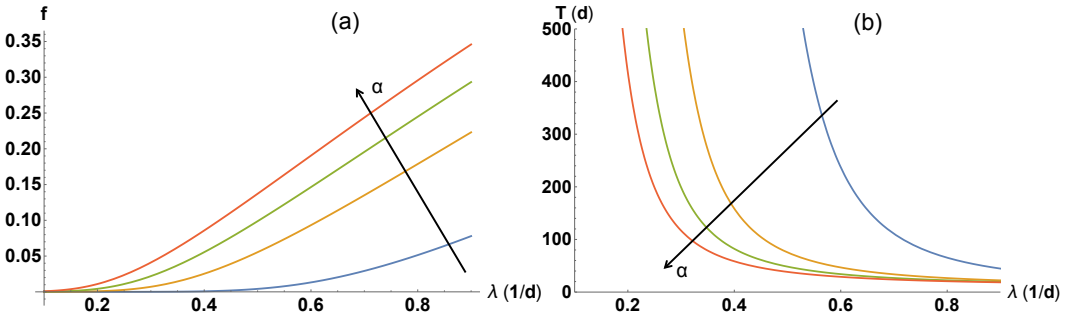

Figure 4. (a) Anoxic fraction of the cycle, f, and (b) duration of the cycle, T, as a function of the frequency of precipitation events, λ, and for different values of mean precipitation depth, α. The values of α, from blue to red line, are 5, 8, 10, and 12 mm. The probability density function for the soil moisture was computed from (Laio et al., 2001), for a silty clay loam soil, average porosity $n = 0.48$, potential evapotranspiration $PET = 4$ mm/d, and hydraulic conductivity $k_h = 14$ cm/d.

3 Soil moisture control on oxic/anoxic cycle

Under field conditions, the frequency and depth of the rainfall events, evapo-transpiration from soil and plants, and soil properties altogether determine the evolution of the soil water and oxygen content, causing the soil to undergo transitions between oxic and anoxic conditions. Since oxygen content exhibits a first dependence on soil moisture (Hall et al., 2013; Calabrese & Porporato, 2019), the average duration of the oxic and anoxic phases, for a given hydro-climate, can be obtained by analyzing the specific time series of soil moisture. Fixing the soil moisture threshold $\hat{s}$ above which soil conditions can be considered anoxic (there are enough anoxic soil microsites to activate anaerobic processes), the average time spent in oxic conditions τ_o then can be calculated as the average time of each excursion below the threshold $\hat{s}$. The average time of each excursion above $\hat{s}$ will be τ_a, the average duration of a oxic/anoxic cycle $T = \tau_a + \tau_o$, and in turn the anoxic fraction of time $f = \tau_a/\tau$.

We show the relationship between the anoxic fraction f, cycle length T and the frequency and mean depth of precipitation (λ and α, respectively) in Figure 4. The curves are drawn for constant soil properties (typical of a silty clay loam) and potential evapotranspiration ($PET = 4$ mm/d) using a stochastic water balance that provides the statistical properties of soil moisture based on rainfall statistics (Laio et al., 2001) (see Appendix A). Because of the high water losses at soil moisture above field capacity, the fraction of time spent in anoxic conditions is generally lower than the one spent in oxic conditions, such that the values of f are below 0.5 (Figure 4). As can be expected, soils are in anoxic conditions on average longer (higher values of f) for high rainfall frequencies accompanied by high average rainfall depths. On the contrary, the whole duration of the cycle, T, decreases with λ as the excursion from oxic to anoxic is more likely to occur. For the realistic range of mean rainfall depth α and frequency λ explored, the length of the full anoxic and oxic cycle T decreases with α, again because it becomes more likely that the soil moisture threshold $\hat{s}$ is crossed. However, for very high mean rainfall depth α and frequency λ the trend in Figure 4 may be inverted as the soil switches to very wet conditions that are in anoxic conditions ($s > \hat{s}$) for most of the time.

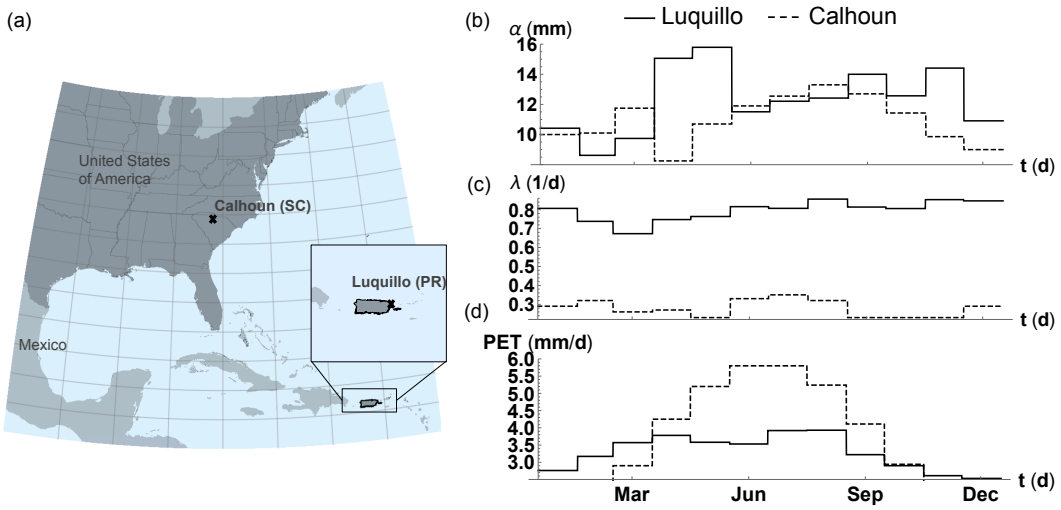

Figure 5. (a) Geographic location of the Luquillo and Calhoun Experimental Forests. (b) Mean depth and (c) frequency of precipitation events per each month. In Luquillo, rainfall statistics are available in Heartsill-Scalley et al. (2007) and Calabrese and Porporato (2019), while in Calhoun they were obtained combining multiple sources ("http://criticalzone.org/calhoun/data/datasets/" and "https://www.usclimatedata.com/climate/south-carolina/united-states/3210"). (d) Monthly average potential evapotranspiration. Values were acquired from the CRU climate dataset (Harris et al., 2014) for Luquillo and from the ORNL DAAC archives data (Vogel & Sankarasubramanian, 2005) for Calhoun.

4 Case studies

4.1 Study areas

The comprehensive hydrological and biogeochemical observations at the tropical forest in Luquillo (Puerto Rico) and at the subtropical forest in Calhoun (South Carolina), which are part of the Critical Zone research network sponsored by the US National Science Foundation, allow us to readily apply the above framework to compare the soil iron dynamics and the potential for iron reduction in these different environments. In Luquillo, we focus on the Bisley watershed, where many Fe cycling studies have been performed. At that site, the mean annual precipitation is about 3.5 m and the vegetation belongs to the Tabonuco forest type (Scatena, 1989). Soils are predominantly Ultisols, formed from volcanic parent material, and belong to the silty clay loam textural class. Calhoun has mean annual precipitation of approximately 1250 mm and vegetation includes mixed hardwood and pine trees. Here soils are also predominantly Ultisols, formed from a granite-gneiss bedrock, and belong to the silt loam textural class (Richter & Markewitz, 2001).

Monthly averaged mean depth and frequency of precipitation as well as potential evapotranspiration for the two sites are illustrated in Figure 5. While Luquillo has a humid tropical climate with only a mild seasonality (slightly reduced rainfall in the winter season), Calhoun has a subtropical climate with marked seasonality in both precipitation and evaporative demand, June and July being the wettest months with also a peak in potential evapotranspiration. Geochemical analysis showed that Luquillo and Calhoun soils have approximately 150 and 45 mmol, respectively, of short-range ordered or low-crystallinity Fe^{III} phases per kilogram of soil (Ginn et al., 2017; Barcellos, Cyle, & Thompson, 2018; Barcellos, 2018). Soil incubation experiments with soil samples from both sites amended with substrate and microbes revealed that reduction rate constants are of the

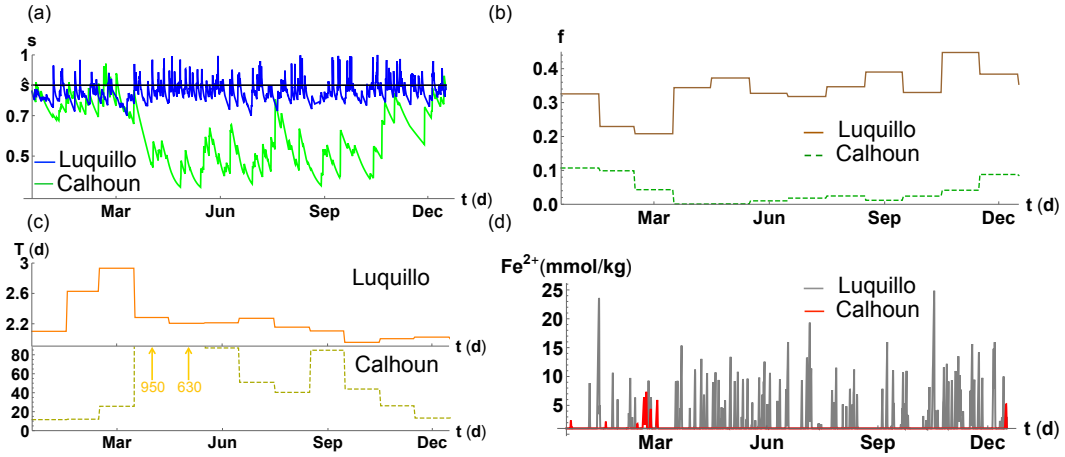

Figure 6. (a) Temporal evolution of soil moisture, simulated by means of the stochastic model in (Laio et al., 2001), in Luquillo (blue line) and Calhoun (green line) over the course of a year. Soils are silty clay loams and silty loams in Luquillo and Calhoun, respectively, with porosity of 0.48. Soil hydrologic properties for the simulation of the soil moisture dynamics from Fernandez-Illescas et al. (2001). Soils are considered to have sufficient anoxic microsites to support Fe reduction for soil moisture levels above $\hat{s} = 0.85$ in Luquillo and $\hat{s} = 0.75$ in Calhoun. (b) Anoxic fraction of the cycle, f, and (c) duration of the cycle, T, for each month computed by means of equations (**??**) and (**??**) in the Appendix. (d) Temporal evolution of Fe^{II} in Luquillo (gray line) and Calhoun (red line) over the course of a year, simulated through equation (1). The reduction and oxidation rate constants are $k_R = 0.1$ and $k_O = 10$ mmol/kg/d, respectively.

order of 10^{-1} d^{-1}, while the oxidation rate constants at 21% O_2 are of the order of 10 d^{-1} (Chen & Thompson, 2017; Ginn et al., 2017).

4.2 Oxic/anoxic cycles and iron reduction

To calculate the temporal dynamics of potential iron reduction (when limited only by the hydrologic regime), we solved equation (1) coupled to a soil water balance that generates a time series of soil moisture levels based on the frequency and mean depth of precipitation events (Figure 6). For Luquillo these rainfall statistics are available in Heartsill-Scalley et al. (2007) and Calabrese and Porporato (2019), while in Calhoun they were obtained combining multiple sources ("http://criticalzone.org/calhoun/data/datasets/" and "https://www.usclimatedata.com/climate/south-carolina/united-states/3210"). The average anoxic fraction f and cycle length T of the oxic/anoxic cycles are then computed for each month from the probability density function of soil moisture (see Appendix A). Note that for each month the parameters f and T are computed assuming stationary climatic conditions. For each month their values thus correspond to oxic/anoxic cycles that would occur if the climatic conditions were stationary and typical of that specific month. As a consequence, it can happen that the value of T is greater than the duration of the month, e.g., $T = 80$ days in Calhoun in September. Of course, these large values of T for a particular month only indicate that it is very unlikely to observe full redox cycles (an Fe oxidation event and an Fe reduction event) in that given month, typically because soil moisture remains below the threshold set.

In Luquillo, the soil moisture frequently crosses the $\hat{s}$ threshold, generating redox cycles of only a few days (2-3 days) throughout the year (Figure 6(a) and (c)). Similarly, the calculated anoxic fraction f remains practically constant during the year and approximately equal to 0.3 (Figure 6(b)). The mild seasonality here is almost not visible in the

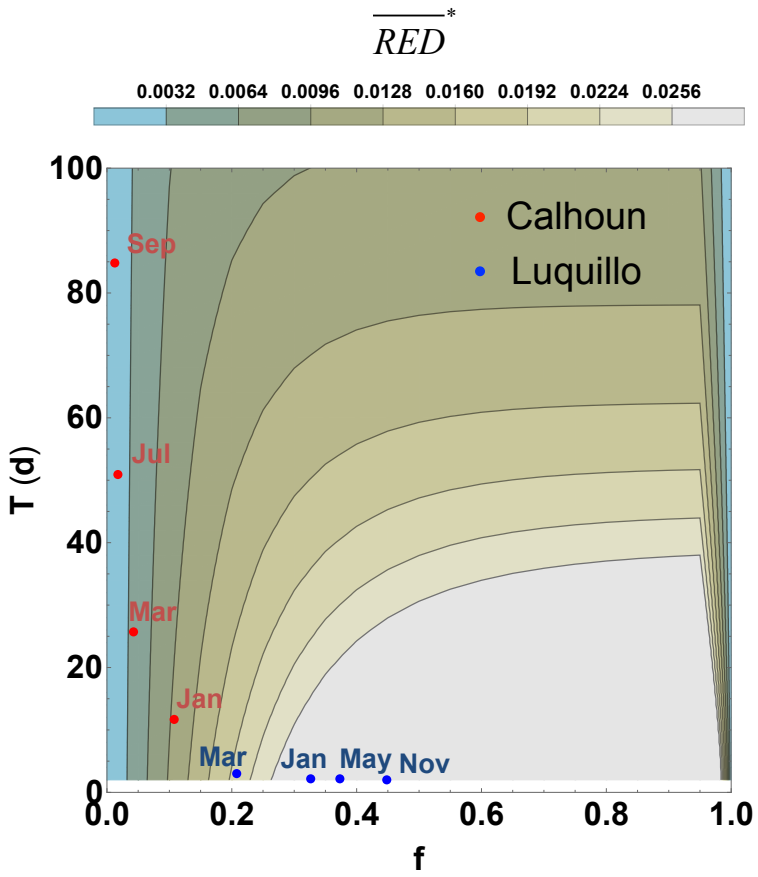

Figure 7. Average and normalized reduction rate per cycle ($\overline{RED}^* = \overline{RED}/Fe^{TOT}$) as a function of the anoxic fraction of the cycle, f, and length of the cycle, T. Corresponding $\overline{RED}^*$ values in different months for Luquillo (blue dots) and Calhoun (red dots). Note that values of T longer than 30 days indicate that a full oxic/anoxic cycle is not expected for that month.

iron dynamics. There are continuous heavy rainfall events that bring soil moisture above the soil moisture threshold $\hat{s}$, stimulating iron reduction, following which the soil returns oxic conditions, triggering rapid Fe^{II} oxidation. As a result, throughout the year Fe^{II} dynamics appears as a series of rapid redox cycles (a reduction followed by the oxidation) initiated by heavy precipitation (Figure 6(d)).

The estimated temporal patterns of the oxic/anoxic cycles and iron reduction are rather different in Calhoun. Compared to Luquillo, the full redox cycles in Calhoun are longer and are affected by the climatic seasonality. Conditions are most favorable for iron cycling only in the late Fall through the early Spring, when the evaporative demand is low. In December and January, for example, the ratio f reaches values of 0.1, much lower than the 0.45 reached in Luquillo in November, while the duration of the cycle reduces to about 10 days (Figure 6(b) and (c)). This results in only a few, long iron redox cycles (Figure 6(d)). From the Spring until the following Fall, the climate favors oxic conditions, with f tending to 0 and T reaching values of over 900 days. After the rapid oxidation in April/May, iron is in fact likely to remain in its oxidized state until the arrival of the following Fall season (Figure 6(d)).

With the above considerations on the different characteristics of the oxic/anoxic cycles in Luquillo and Calhoun, the pace of iron cycling can be quantified by means of

the average reduction rate. To use an index of iron reduction that depends only on the oxic/anoxic cycle and that can be used to compare the two study sites, we computed the average reduction rate $\overline{RED}$, Fe reduced per cycle divided by the duration of the cycle, and normalized it by the total short range ordered Fe content, $\overline{RED}^* = \overline{RED}/Fe^{TOT}$. The term $\overline{RED}^*$ is thus analyzed as a function of the fraction in anoxic conditions f and the overall duration of the cycle T (Figure 7). For the reduction and oxidation rate constants found in these forests, the optimum oxic/anoxic cycle has an anoxic fraction $f \approx 0.8$ and a cycle length T shorter than 10 days. The humid tropical climate in Luquillo guarantees a high potential for iron reduction throughout the year, with only slightly less favorable conditions in the spring (blue dots in Figure 5(d)). Differently from Luquillo, the seasonal climate in Calhoun is largely reflected in the soil redox conditions. As we have seen above, the Fall until the beginning of the Spring is the period with the highest potential for iron reduction. Indeed, January has an almost optimal oxic/anoxic cycle for iron reduction. On the contrary, conditions are far from favorable in the late Spring and in the summer, when due to lower precipitation and high evapotranspiration, respectively, oxic conditions tend to persist.

5 Discussion

The high potential of iron reduction predicted here, which is consistent with previous reported rates (Yang & Liptzin, 2015; Hall et al., 2013; Barcellos, Cyle, & Thompson, 2018), suggests that a large portion of soil organic matter potentially can be decomposed through iron reduction rather than aerobic decomposition, making iron fundamental for the functioning of these ecosystems. In humid tropical forests, such as Luquillo, iron redox cycles occur throughout the year because the high rainfall can continuously sustain fluctuations in oxic/anoxic conditions. Experimental (Dubinsky et al., 2010) and modeling (Calabrese & Porporato, 2019) studies in fact estimated that up to 40% of organic matter decomposition could be attributed to iron reduction. In subtropical forests, such as Calhoun in the Southeastern Piedmont in USA, the marked climatic seasonality greatly controls iron reduction, which is favored only in those months with higher rainfall and lower evaporative demand. This finding is supported by recent experiments in Calhoun, where potential of iron reduction was measured over the course of a year by means of steel IRIS (Indicator of Reduction of Iron in Soils) probes (Hodges et al., 2019).

Other than impacting directly the carbon cycle, iron redox cycling also affects the productivity of plants (Colombo et al., 2014; Calabrese & Porporato, 2019), because iron is a micro-nutrient essential for plants to support their physiological processes (e.g., photosynthesis) and is directly related to the bioavailability in soils of phosphorous, which tends to be adsorbed to iron oxides with high surface area (Miller et al., 2001; Chacon et al., 2006; Gross et al., 2018; E. M. Herndon et al., 2019; Khan et al., 2019). It is thus the in-situ hydro-climate that controls the availability of these two nutrients. Wet conditions favor iron reduction and thus more Fe^{II} and P in the soil solution. If conditions are constantly wet, however, iron may almost completely dissolve in water, causing plants to uptake large amounts of iron that result toxic to their cells (Foy et al., 1978). Dry conditions, on the contrary, make these nutrients unavailable because they favor iron oxidation, with formation of iron oxyhydroxides (Fe^{III}), on which phosphorous can be strongly adsorbed. Interestingly, plants are able to cope with iron deficient or toxic conditions by affecting, for example, the redox potential in the rhizosphere (Guerinot & Yi, 1994; Rout & Sahoo, 2015), thus exerting a feedback on the iron redox dynamics. Variations in rainfall frequency and depth, resulting from climate changes, call for modeling frameworks able to quantify the coupled soil iron-plants dynamics, which is of interest not only to predict the future response of natural ecosystems, but also to refine irrigation and fertilization strategies in agroecosystems, to limit the utilization of resources while guaranteeing food security (FAO, 2015).

A deeper understanding of iron cycling is required also to reduce the uncertainty in the carbon budget, particularly in tropical and temperate forests (Bailey et al., 2018; Kramer & Chadwick, 2018). The former contain some 20% of global soil carbon and have among the highest rates of greenhouse gas emissions (Jobbágy & Jackson, 2000; Malhi & Grace, 2000), while the latter (e.g., the eastern USA) have high potential for soil and plant carbon storage, given that these forests have been recovering after historically being deforested (Bonan, 2008). Because iron cycling in upland soils is driven by the wetting and drying of soils upon the intermittent arrival of precipitation, for a realistic and more accurate description of these dynamics, Earth system and climate models need to account for the temporal oxic/anoxic transitions driven by hydro-climatic fluctuations, especially when investigating future soil carbon storage and its feedback on the long-term climate.

6 Conclusions

Through the minimalist model of iron redox dynamics presented here, we relate the potential rates of iron reduction to the hydro-climatic variability through its influence on changes in soil moisture and predicted oxic and anoxic conditions. The study showed that hydro-climatic variability may favor or inhibit iron reduction, depending on how closely the resulting oxic/anoxic cycle approaches the 'optimal' oxic/anoxic cycle. By relating the rate of the soil iron cycle to hydro-climatic fluctuations, this analysis also paves the way for a global identification of hot spots of iron reduction, in which climatic features are highly favorable, and for prediction of future trends in organic matter decomposition. We also believe that these results represent an important step toward an improved representation of biogeochemical processes, especially anaerobic processes (e.g., Zheng et al. (2019) and Calabrese and Porporato (2019)), in Earth system models (e.g., Hurrell et al. (2013)).

Acknowledgments

This work was supported through the National Science Foundation (NSF) grants EAR-1331846 and FESD-1338694 and the Carbon Mitigation Initiative at Princeton University. The data used in this paper are properly cited throughout the manuscript.

References

Bailey, V. L., Bond-Lamberty, B., DeAngelis, K., Grandy, A. S., Hawkes, C. V., Heckman, K., ... others (2018). Soil carbon cycling proxies: Understanding their critical role in predicting climate change feedbacks. *Global change biology*, *24*(3), 895–905.

Barcellos, D. (2018). *Biogeochemical cycling of iron and carbon in humid (sub) tropical forest soils under fluctuating redox conditions* (Unpublished doctoral dissertation). University of Georgia.

Barcellos, D., Cyle, K. T., & Thompson, A. (2018). Faster redox fluctuations can lead to higher iron reduction rates in humid forest soils. *Biogeochemistry*, *137*(3), 367–378.

Barcellos, D., OConnell, C., Silver, W., Meile, C., & Thompson, A. (2018). Hot spots and hot moments of soil moisture explain fluctuations in iron and carbon cycling in a humid tropical forest soil. *Soil Systems*, *2*(4), 59.

Bhattacharyya, A., Campbell, A. N., Tfaily, M. M., Lin, Y., Kukkadapu, R. K., Silver, W. L., ... Pett-Ridge, J. (2018). Redox fluctuations control the coupled cycling of iron and carbon in tropical forest soils. *Environmental science & technology*, *52*(24), 14129–14139.

Bishop, M. E., Glasser, P., Dong, H., Arey, B., & Kovarik, L. (2014). Reduction and immobilization of hexavalent chromium by microbially reduced fe-bearing clay

minerals. *Geochimica et Cosmochimica Acta*, *133*, 186–203.
Bonan, G. B. (2008). Forests and climate change: forcings, feedbacks, and the climate benefits of forests. *science*, *320*(5882), 1444–1449.
Borch, T., Kretzschmar, R., Kappler, A., Cappellen, P. V., Ginder-Vogel, M., Voegelin, A., & Campbell, K. (2009). Biogeochemical redox processes and their impact on contaminant dynamics. *Environmental science & technology*, *44*(1), 15–23.
Brady, N. C., & Weil, R. R. (2016). *The nature and properties of soils*. Pearson.
Buettner, S. W., Kramer, M. G., Chadwick, O. A., & Thompson, A. (2014). Mobilization of colloidal carbon during iron reduction in basaltic soils. *Geoderma*, *221*, 139–145.
Calabrese, S., & Porporato, A. (2019). Impact of ecohydrological fluctuations on iron-redox cycling. *Soil Biology and Biochemistry*.
Chacon, N., Silver, W. L., Dubinsky, E. A., & Cusack, D. F. (2006). Iron reduction and soil phosphorus solubilization in humid tropical forests soils: the roles of labile carbon pools and an electron shuttle compound. *Biogeochemistry*, *78*(1), 67–84.
Chen, C., & Thompson, A. (2017). Ferrous iron oxidation under varying po2 levels: the effect of fe (iii)/al (iii) oxide minerals and organic matter. *Environmental science & technology*, *52*(2), 597–606.
Colombo, C., Palumbo, G., He, J.-Z., Pinton, R., & Cesco, S. (2014). Review on iron availability in soil: interaction of fe minerals, plants, and microbes. *Journal of Soils and Sediments*, *14*(3), 538–548.
Couture, R.-M., Charlet, L., Markelova, E., Made, B., & Parsons, C. T. (2015). On–off mobilization of contaminants in soils during redox oscillations. *Environmental science & technology*, *49*(5), 3015–3023.
Dubinsky, E. A., Silver, W. L., & Firestone, M. K. (2010). Tropical forest soil microbial communities couple iron and carbon biogeochemistry. *Ecology*, *91*(9), 2604–2612.
FAO, I. (2015). Status of the worlds soil resources (swsr)–main report. *Food and agriculture organization of the United Nations and intergovernmental technical panel on soils, Rome, Italy*, *650*.
Fernandez-Illescas, C. P., Porporato, A., Laio, F., & Rodriguez-Iturbe, I. (2001). The ecohydrological role of soil texture in a water-limited ecosystem. *Water Resources Research*, *37*(12), 2863–2872.
Foy, C., Chaney, R. t., & White, M. (1978). The physiology of metal toxicity in plants. *Annual review of plant physiology*, *29*(1), 511–566.
Ginn, B., Meile, C., Wilmoth, J., Tang, Y., & Thompson, A. (2017). Rapid iron reduction rates are stimulated by high-amplitude redox fluctuations in a tropical forest soil. *Environmental Science & Technology*, *51*(6), 3250–3259.
Gross, A., Pett-Ridge, J., & Silver, W. (2018). Soil oxygen limits microbial phosphorus utilization in humid tropical forest soils. *Soil Systems*, *2*(4), 65.
Guerinot, M. L., & Yi, Y. (1994). Iron: nutritious, noxious, and not readily available. *Plant Physiology*, *104*(3), 815.
Hall, S. J., McDowell, W. H., & Silver, W. L. (2013). When wet gets wetter: decoupling of moisture, redox biogeochemistry, and greenhouse gas fluxes in a humid tropical forest soil. *Ecosystems*, *16*(4), 576–589.
Han, L., Sun, K., Keiluweit, M., Yang, Y., Yang, Y., Jin, J., ... Xing, B. (2019). Mobilization of ferrihydrite-associated organic carbon during fe reduction: Adsorption versus coprecipitation. *Chemical Geology*, *503*, 61–68.
Harris, I., Jones, P. D., Osborn, T. J., & Lister, D. H. (2014). Updated high-resolution grids of monthly climatic observations–the cru ts3. 10 dataset. *International journal of climatology*, *34*(3), 623–642.
Heartsill-Scalley, T., Scatena, F. N., Estrada, C., McDowell, W., & Lugo, A. E. (2007). Disturbance and long-term patterns of rainfall and throughfall nu-

trient fluxes in a subtropical wet forest in puerto rico. *Journal of Hydrology*, *333*(2-4), 472–485.

Henderson, R., Kabengi, N., Mantripragada, N., Cabrera, M., Hassan, S., & Thompson, A. (2012). Anoxia-induced release of colloid-and nanoparticle-bound phosphorus in grassland soils. *Environmental science & technology*, *46*(21), 11727–11734.

Herndon, E., AlBashaireh, A., Singer, D., Chowdhury, T. R., Gu, B., & Graham, D. (2017). Influence of iron redox cycling on organo-mineral associations in arctic tundra soil. *Geochimica et Cosmochimica Acta*, *207*, 210–231.

Herndon, E. M., Kinsman-Costello, L., Duroe, K. A., Mills, J., Kane, E. S., Sebestyen, S. D., ... Wullschleger, S. D. (2019). Iron (oxyhydr) oxides serve as phosphate traps in tundra and boreal peat soils. *Journal of Geophysical Research: Biogeosciences*, *124*(2), 227–246.

Hodges, C., Mallard, J., Markewitz, D., Barcellos, D., & Thompson, A. (2019). Seasonal and spatial variation in the potential for iron reduction in soils of the southeastern piedmont of the us. *Catena*, *180*, 32–40.

Hurrell, J. W., Holland, M. M., Gent, P. R., Ghan, S., Kay, J. E., Kushner, P. J., ... others (2013). The community earth system model: a framework for collaborative research. *Bulletin of the American Meteorological Society*, *94*(9), 1339–1360.

Jobbágy, E. G., & Jackson, R. B. (2000). The vertical distribution of soil organic carbon and its relation to climate and vegetation. *Ecological applications*, *10*(2), 423–436.

Khan, I., Fahad, S., Wu, L., Zhou, W., Xu, P., Sun, Z., ... others (2019). Labile organic matter intensifies phosphorous mobilization in paddy soils by microbial iron (iii) reduction. *Geoderma*, *352*, 185–196.

Kramer, M. G., & Chadwick, O. A. (2018). Climate-driven thresholds in reactive mineral retention of soil carbon at the global scale. *Nature Climate Change*, *8*(12), 1104.

LaCroix, R. E., Tfaily, M. M., McCreight, M., Jones, M. E., Spokas, L., & Keiluweit, M. (2019). Shifting mineral and redox controls on carbon cycling in seasonally flooded mineral soils. *Biogeosciences*, *16*(13), 2573–2589.

Laio, F., Porporato, A., Ridolfi, L., & Rodriguez-Iturbe, I. (2001). Plants in water-controlled ecosystems: active role in hydrologic processes and response to water stress: Ii. probabilistic soil moisture dynamics. *Advances in Water Resources*, *24*(7), 707–723.

LaRowe, D. E., & Van Cappellen, P. (2011). Degradation of natural organic matter: a thermodynamic analysis. *Geochimica et Cosmochimica Acta*, *75*(8), 2030–2042.

Lovley, D. R. (1991). Dissimilatory fe (iii) and mn (iv) reduction. *Microbiological reviews*, *55*(2), 259–287.

Malhi, Y., & Grace, J. (2000). Tropical forests and atmospheric carbon dioxide. *Trends in Ecology & Evolution*, *15*(8), 332–337.

Miller, A. J., Schuur, E. A., & Chadwick, O. A. (2001). Redox control of phosphorus pools in hawaiian montane forest soils. *Geoderma*, *102*(3-4), 219–237.

Morel, F. M., Hering, J. G., et al. (1993). *Principles and applications of aquatic chemistry*. John Wiley & Sons.

Oertel, C., Matschullat, J., Zurba, K., Zimmermann, F., & Erasmi, S. (2016). Greenhouse gas emissions from soilsa review. *Chemie der Erde-Geochemistry*, *76*(3), 327–352.

Richter, D. D., & Markewitz, D. (2001). Understanding soil change. *Understanding Soil Change, by Daniel D. Richter, Jr and Daniel Markewitz and Foreword by William A. Reiners and Pedro Sánchez, pp. 272. ISBN 0521771714. Cambridge, UK: Cambridge University Press, June 2001.*, *1*.

Roden, E. E., & Wetzel, R. G. (1996). Organic carbon oxidation and suppression of

methane production by microbial fe (iii) oxide reduction in vegetated and unvegetated freshwater wetland sediments. *Limnology and Oceanography*, *41*(8), 1733–1748.

Rout, G. R., & Sahoo, S. (2015). Role of iron in plant growth and metabolism. *Reviews in Agricultural Science*, *3*, 1–24.

Scatena, F. N. (1989). An introduction to the physiography and history of the bisley experimental watersheds in the luquillo mountains of puerto rico. *Gen. Tech. Rep. SO-72. New Orleans, LA: US Dept of Agriculture, Forest Service, Southern Forest Experiment Station. 22 p.*, *72*.

Stucki, J. W. (2011). A review of the effects of iron redox cycles on smectite properties. *Comptes Rendus Geoscience*, *343*(2-3), 199–209.

Thompson, A., Chadwick, O. A., Rancourt, D. G., & Chorover, J. (2006). Iron-oxide crystallinity increases during soil redox oscillations. *Geochimica et Cosmochimica Acta*, *70*(7), 1710–1727.

Todd-Brown, K. E., Hopkins, F. M., Kivlin, S. N., Talbot, J. M., & Allison, S. D. (2012). A framework for representing microbial decomposition in coupled climate models. *Biogeochemistry*, *109*(1-3), 19–33.

Vermeire, M.-L., Bonneville, S., Stenuit, B., Delvaux, B., & Cornélis, J.-T. (2019). Is microbial reduction of fe (iii) in podzolic soils influencing c release? *Geoderma*, *340*, 1–10.

Vogel, R., & Sankarasubramanian, A. (2005). *Monthly climate data for selected usgs hcdn sites, 1951-1990, r1.* ORNL Distributed Active Archive Center. Retrieved from `http://daac.ornl.gov/cgi-bin/dsviewer.pl?ds_id=810` doi: 10.3334/ORNLDAAC/810

Wang, Y., Liu, C., Peng, A., & Gu, C. (2019). Formation of hydroxylated polychlorinated diphenyl ethers mediated by structural fe (iii) in smectites. *Chemosphere*, *226*, 94–102.

Weiss, J. V., Emerson, D., & Megonigal, J. P. (2004). Geochemical control of microbial fe (iii) reduction potential in wetlands: comparison of the rhizosphere to non-rhizosphere soil. *FEMS Microbiology Ecology*, *48*(1), 89–100.

Weiss, J. V., Emerson, D., & Megonigal, J. P. (2005). Rhizosphere iron (iii) deposition and reduction in a l.-dominated wetland. *Soil Science Society of America Journal*, *69*(6), 1861–1870.

Yang, W. H., & Liptzin, D. (2015). High potential for iron reduction in upland soils. *Ecology*, *96*(7).

Yu, H.-Y., Li, F.-B., Liu, C.-S., Huang, W., Liu, T.-X., & Yu, W.-M. (2016). Iron redox cycling coupled to transformation and immobilization of heavy metals: implications for paddy rice safety in the red soil of south china. In *Advances in agronomy* (Vol. 137, pp. 279–317). Elsevier.

Zheng, J., Thornton, P. E., Painter, S. L., Gu, B., Wullschleger, S. D., & Graham, D. E. (2019). Modeling anaerobic soil organic carbon decomposition in arctic polygon tundra: insights into soil geochemical influences on carbon mineralization. *Biogeosciences*, *16*(3), 663–680.